Preprints of the 21st IFAC World Congress (Virtual)
Berlin, Germany, July 12-17, 2020

Modelling and Simulation of the Human Cardiovascular System by Differential Hybrid Petri Net

André A. Jorge*, Marcosiris A. O. Pessoa*, Fabrício Junqueira*, Luis A. M. Riascos, Diolino J. Santos Filho*, Paulo E. Miyagi***

**Escola Politecnica da Universidade de Sao Paulo, Brazil*
(e-mails: andre.anjorge@gmail.com, marcosiris@usp.br, fabri@usp.br, diolinos@usp.br, pemiyagi@usp.br)
***Universidade Federal do ABC, Brazil*
(e-mail: luis.riascos@ufabc.edu.br)

Abstract: Clinical data surveys indicate a significant number of deaths deriving from diseases in the human cardiovascular system (HCS). This is one of the main motivations for identifying problems in this system and ways for solving them totally or partially. In this work, HCS is modeled as a hybrid system (discrete event systems combined with systems of continuous variables) for a more detailed characterization of this system functioning, by applying the formalism of the Differential Hybrid Petri Net (DHPN). The analysis of this model, using Matlab®/Simulink, presented consistent results when compared with clinical data, regarding physiological variables, such as blood pressure and blood flow rate, indicating the validity of this model.

Keywords: Human cardiovascular system, Hybrid systems, Differential hybrid Petri nets, Lumped parameter model, Blood pressure, Blood flow rate.

Nomenclature

C	Capacitance
$\mathcal{C}$	Complacency of the vessel wall
D	Diode (Valve)
E	Elastance
HR	Heart Rate
I	Electrical current
K	Coefficient
L	Inductance
$\mathcal{L}$	Blood inertia
P	Blood pressure
Q	Blood flow rate
q	Charge
R	Electrical resistance
$\mathcal{R}$	Viscous flow resistance
t	Time
V	Volume
v	Voltage

Subscripts

0	Initial Value; Offset Value
A	Aorta
AV	Aortic Valve
LA	Left Atrium
LV	Left Ventricle
MAX	Maximum Value
MIN	Minimum Value
MV	Mitral Valve
PA	Pulmonary Artery
PAR	Pulmonary Arterioles
PAS	Pulmonary Arteries
PAV	Pulmonary Vein
PC	Pulmonary Capillaries
PV	Pulmonary Valve
PVS	Pulmonary Veins
RA	Right Atrium
RS	Repeating Sequence
RV	Right Ventricle
SA	Systemic Arteries
SAR	Systemic Arterioles
SC	Systemic Capillaries
SV	Systemic Veins
TV	Tricuspid Valve
VC	Vena Cava

1. INTRODUCTION

According to the World Health Organization (2017), cardiovascular diseases (CVDs) are still the number one cause of death globally; more people die annually from CVDs than from any other cause. Thus, many studies for identifying problems in the human cardiovascular system (HCS) and ways for solving them, totally or partially, have increased over the years (Jorge et al., 2018, 2019a, 2019b).

The laws of blood fluid dynamics, called hemodynamic, govern the cardiovascular system. Hemodynamic may be described by three parameters: blood flow (cardiac output), blood pressure and vascular resistance. The measurement of these hemodynamic parameters is the foundation for diagnosing different CVDs (Westerhof et al., 2005).

Since there is a growing demand for restrictions on *in vivo* testing for the medical equipment industry, including the case of animal testing (Watanabe et al., 2014), new strategies and platforms for *in vitro* tests and tools for evaluating implantable medical devices, such as ventricular assist devices (VADs), must be considered (Jorge et al., 2018, 2019a, 2019b).

Knowing that any closed fluid system has an analogy with electrical circuits (Westerhof et al., 2005), the cardiovascular system may be considered analogous to electrical circuits. Thus, lumped parameter models, known as 0D model or electrical circuits, of the HCS are an appropriate method to obtain several hemodynamic parameters of the blood circulation (Formaggia et al., 2009; Rahman and Haque, 2012; Gul, 2016).

Hybrid systems are defined as systems in which state variables of a continuous and discrete nature are simultaneously found. The evolution of the system may occur partially as a function of time and/or as a function of the discrete event occurrence. This means that, in a hybrid system, subsystems belonging to the two classes presented coexist simultaneously (Villani et al., 2007).

In general, the approaches to the modeling of hybrid systems consist in extensions of continuous models, such as ordinary differential equations, in which variables whose value may be modified in a discontinuous way in time, are included. Other approaches consist in modifying modeling techniques applied to discrete event systems, whereby new elements are introduced to represent the continuous dynamics of the system, such as in the models based on Hybrid Petri net (David and Alla, 2010). In addition, there are also intermediate approaches that combine models of continuous systems, described by differential equations, and discrete systems, described by finite automata or Petri net (Giua and Silva, 2017; Boussif and Ghazel, 2018), in which an interface is established for the communication between the two types of models (Jorge et al., 2019a, 2019b). However, these works (Jorge et al., 2019a, 2019b) have a limitation to modelling cardiovascular diseases, considered as discrete events, due to the modelling approach used (0D model).

This work proposes a model for the HCS applying the formalism of the Differential Hybrid Petri Net (DHPN), using the equations derived from the lumped parameter model previously developed and presented in (Jorge et al., 2019a, 2019b). The goal of this contribution is proposing a valid model of the HCS to study the behaviour of this system, taking into account the interactions among their dynamics (continuous system combined with discrete events). This proposed model was simulated and analysed using Matlab®/Simulink. The focus lies on the analysis and comparison of the blood flow rate and blood pressure from clinical data with simulated data.

2. METHODOLOGY

In Jorge et al. (2019a, 2019b), the lumped parameter model or the 0D model was applied to model the HCS, since this technique represents physiological variables, such as blood pressure, blood flow rate, viscous flow resistance and others, of the blood circulation system, presenting an immediate solution.

According to Formaggia, Quarteroni and Veneziani (2009) and Rahman and Haque (2012), each segment of a blood vessel may be represented by a resistor-inductor-capacitor (RLC) electrical circuits (0D model). Table 1 summarizes the relationship among the variables considered (Gul, 2016; Malatos, Raptis and Xenos, 2016; Jorge et al., 2019a, 2019b).

Table 1. Analogy among elements of the fluid dynamics, physiological variables and electrical system.

Fluid Dynamics	Physiologyical Variables	Electrical System
Pressure	Blood pressure (P)	Voltage (v)
Flow rate	Blood flow rate (Q)	Current (I)
Volume	Blood volume (V)	Charge (q)
Viscosity	Viscous flow resistance ($\mathcal{R}$)	Resistance (R)
Inertance	Blood inertia ($\mathcal{L}$)	Inductance (L)
Elastic coefficient	Complacency ($\mathcal{C}$)	Capacitance (C)

This model considers the blood leaves the left ventricle, flows through the systemic circulation (body except lungs) into the right part of the heart (atrium and ventricle) and from there through the vessels of the pulmonary circulation (lungs) back into the left atrium and ventricle (Guyton and Hall, 2011) and (Tortora and Derrickson, 2014).

The parameter values for the proposed lumped parameter model (Fig. 1) are derived from (Korakianitis and Shi, 2006a, 2006b) and adjusted for this model. However, several difficulties make parameter setting a challenging task, such as: the invasive nature of many of the measurements, restricted access to the required measurement sites due to anatomical configuration, practical difficulties in the orientation of flow probes (particularly invasive ones), difficulties in synchronizing pressure and flow data (particularly when they are not measured simultaneously), limited precision in the pressure/flow sensors, all of which contribute to the accuracy of the model parameters (Shi, Lawford and Hose, 2011). Perhaps more important, the data available of the pressure measurement provides only part of the information needed to estimate the model parameters. Thus, it is necessary to develop more accurate and efficient techniques to optimize the parameter setting in lumped parameter models (Jorge et al., 2019a, 2019b).

2.1 Human Cardiovascular System

The model of pulsatile human blood circulation consists of a pumping heart coupled to lumped descriptions of the systemic and the pulmonary circulation (loop). The ventricles are guided by a pair of time-varying elastance functions, whereas the two atria are purely passive chambers. In addition, there are four heart valves (mitral, aortic, tricuspid and pulmonary) in these chambers, as shown in Fig. 1. The valves allow a small amount of volume to flow back into the left and right atria and ventricles before closure is completed. When the left atrial pressure exceeds the left ventricular pressure, the mitral valve (*MV*) opens and the left ventricle is filled with blood. After that, when left ventricular pressure exceeds the root aortic pressure, the aortic valve (*AV*) opens and blood flows through the systemic circulation, consisting of aorta (*A*), systemic arteries (*SA*), systemic arterioles (*SAR*), systemic capillaries (*SC*), systemic veins (*SV*) and vena cava (*VC*). The veins return the blood to the passive right atria. Next, when the right atrial pressure exceeds the

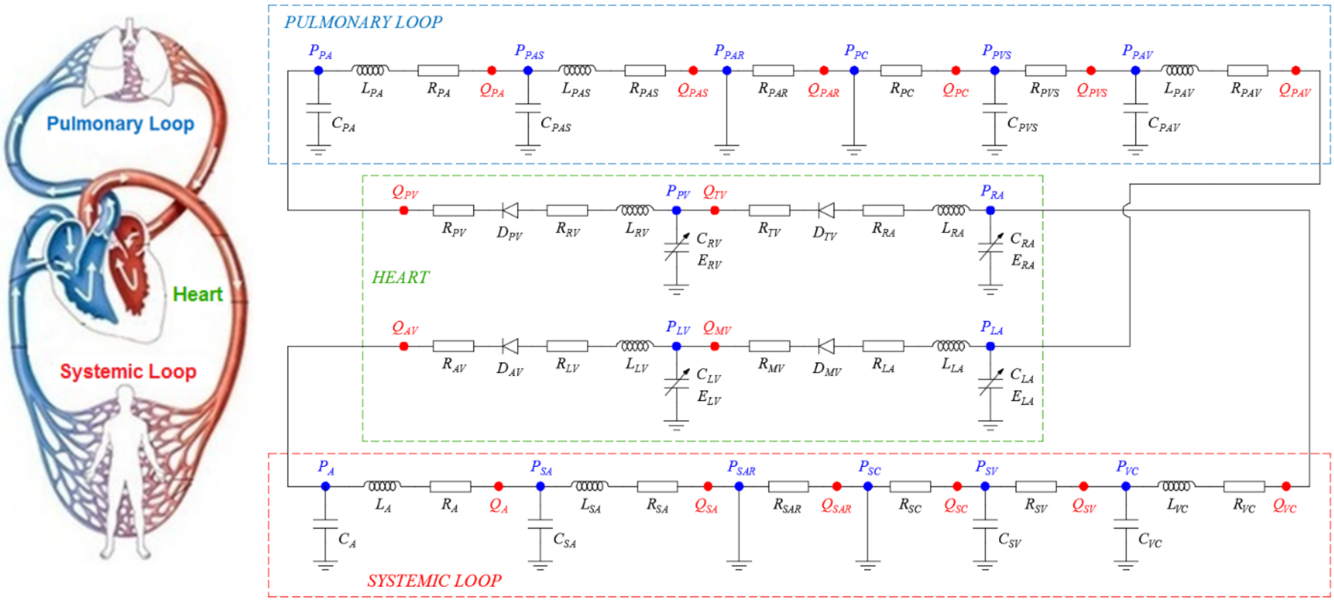

Fig. 1. Main components of the 0D model for the human cardiovascular system.

right ventricular pressure, the tricuspid valve (*TV*) opens and the right ventricle is filled with blood. Then, when the right ventricular pressure exceeds the root pulmonary artery pressure, the pulmonary valve (*PV*) opens and blood flows through the pulmonary circulation, consisting of pulmonary artery (*PA*), pulmonary arteries (*PAS*), pulmonary arterioles (*PAR*), pulmonary capillaries (*PC*), pulmonary veins (*PVS*) and pulmonary vein (*PAV*), returning to the left atrium and starting a new cycle.

2.1.1 Heart

The cardiac contractile properties of the atria and ventricles are assumed to be defined by time-varying elastance functions. The relation between left ventricular cavity pressure (P_{LV}) and ventricular volume (V_{LV}) is described by (Ferreira et al., 2005):

$$P_{LV} = E_{LV}(t)\left(V_{LV} - V_{LV\_0}\right), \quad (1)$$

where V_{LV_0} represents the left ventricular volume at zero pressure. The elastance function $E(t)$ is given by (Ferreira et al., 2005):

$$E(t) = (E_{max} - E_{min})\left(1.55\left[\frac{\left(\frac{t_n}{0.7}\right)^{1.9}}{1+\left(\frac{t_n}{0.7}\right)^{1.9}}\right]\left[\frac{1}{1+\left(\frac{t_n}{1.17}\right)^{21.9}}\right]\right) + E_{min} \quad (2)$$

In (2), $t_n = t/T_{max}$, $T_{max} = 0.2 + 0.15.t_c$ and t_c is the cardiac cycle interval, i.e, $t_c = 60/HR$, where HR is the heart-rate. Notice that constants E_{max} and E_{min} are related to the end-systolic pressure volume relationship (ESPVR) and the end-diastolic pressure volume relationship (EDPVR), respectively (Ferreira et al., 2005).

The flow rate in the aortic valve is described by:

$$\begin{cases} \dfrac{dQ_{AV}}{dt} = \dfrac{P_{LV} - P_A - (R_{LV} + R_{AV})Q_{AV}}{L_{LV}}, & \text{aortic valve is open} \\ Q_{AV} = 0, & \text{aortic valve is closed} \end{cases} \quad (3)$$

The behaviour of the left and right atria, the right ventricle and the other valves are modeled by a similar description.

2.1.2 Notation for the Cardiovascular Model

The notation used in the electrical analogy of the cardiovascular system is the same adopted by Formaggia, Quarteroni and Veneziani (2009). From Fig. 2, the governing equations associated to this generic single segment of a blood vessel are given by (Blanco and Feijóo, 2010):

$$L\frac{dQ_o}{dt} + RQ_o = P_i - P_o, \quad (4)$$

$$C\frac{d}{dt}(P_i - P_{ex}) = Q_i - Q_o, \quad (5)$$

where P_i and P_o are the input and output pressures, P_{ex} is the external pressure, Q_i and Q_o are the blood inflow and outflow.

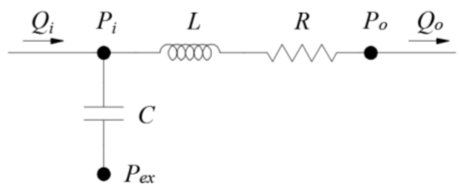

Fig. 2. Single segment of a blood vessel circuit representation.

2.2 Differential Hybrid Petri Nets

A DHPN is composed of two types of places and two types of transitions: discrete places and transitions, differential places and transitions, see Fig. 3. A DHPN has three types of arcs: normal arc, test arc and inhibitor arc. The normal arc and the inhibitor arc can be used to connect discrete elements, and the test arc is used for connecting differential places and discrete transitions.

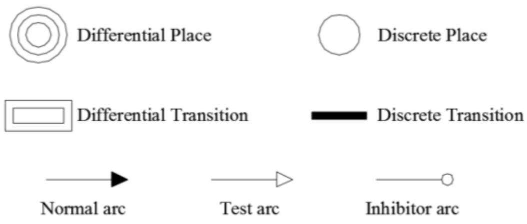

Fig. 3. Places and transitions of DHPN.

A DHPN is defined by a 14 tuple (P_D, T_D, P_D, T_{DF}, X, A_N, A_I, A_T, P_{re}, P_{os}, Γ, H, J, M_0), where (Sousa and Lima, 2008; Yu, Dou and Li, 2016):

$P_D = \{P_1, P_2, \ldots, P_n\}$ is a finite and non-empty set of discrete places, which represents the operation modes of all units;

$T_D = \{T_1, T_2, \ldots, T_n\}$ is a finite and non-empty set of discrete transitions, which represents the event-triggered switching behaviours;

$P_{DF} = \{P_{1f}, P_{2f}, \ldots, P_{nf}\}$ is a finite and non-empty set of differential places, which describes the continuous states of all units;

$T_{DF} = \{T_{1f}, T_{2f}, \ldots, T_{nf}\}$ is a finite and non-empty set of differential transitions, which represents the dynamic behaviours;

$P = P_D \cup P_{DF}$, $T = T_D \cup T_{DF}$, $P \cap T = \emptyset$ e $P \cup T \neq \emptyset$;

$X = [x_1, x_2, \ldots, x_n]^T$, is a continuous state vector of P_{DF};

$A_N \subseteq ((P_D \times T_D) \cup (T_D \times P_D)) \cup ((P_D \times T_{DF}) \cup (TDF \times PD))$ is a set of normal arcs;

$A_I \subseteq (P_D \times T_D)$ is a set of inhibitor arcs;

$A_T \subseteq (P_D \times T_D) \cup (T_D \times P_{DF})$ is a set of test arcs;

$Pre\ (P_i, T_j)\ P_D \times T_D \rightarrow \mathrm{N}$ is called the predecessor function, which defines the normal arcs of a place to a transition;

$Pos\ (P_i, T_j)\ P_D \times T_D \rightarrow \mathrm{N}$ is called a successor function, which defines the normal arcs of a transition to a place;

Γ is a timing map for the discrete transitions, by which the minimal switching interval can be defined;

$H_{Pi,Tj} : P_{DF} \times T_D \rightarrow X$ is a junction function associated with the test arc, which connects a differential input place P_i to a discrete transition T_j;

$J_{Tj,Pi} : T_D \times P_{DF} \rightarrow X$ is an enabling function associated with the test arc, which connects a transition ($T_j \in T_D$) to a differential output place ($P_i \in P_{DF}$);

$M_0\,(t) : \mathrm{P} \rightarrow \mathrm{N}$, represents the initial marking of the net in $t = 0$.

A model proposal for the HCS, by applying the formalism of the DHPN, was developed, as presented in Fig. 4. In this model, the enabling functions $HP_1,T_{17} : P_{LA} \geq P_{LV}$ and $HP_2,T_{18} : P_{LA} < P_{LV}$ enable opening and closing the Mitral Valve, depending on when the left atrium pressure is greater or equal or less than the left ventricle pressure, respectively. From the differential equations of the 0D model, derived by manipulation of (4) and (5), the differential continuous state vector of T_{DF} and the continuous state vector of P_{DF} are obtained, as indicated in Fig. 4. The other enabling functions for the other valves and the other differential continuous state vectors have a similar approach.

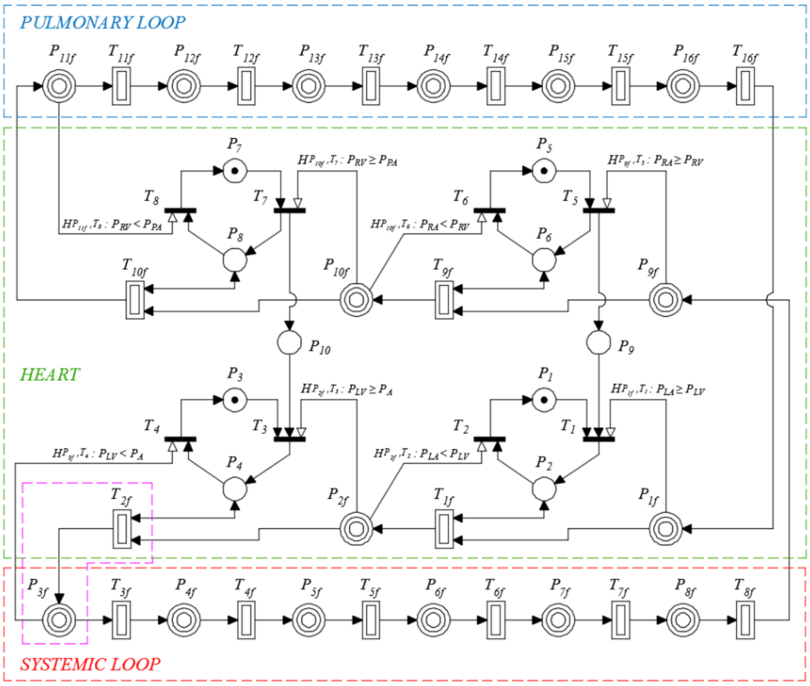

P_{DF}	*Continuous Dynamics*
P_{1f}	Left Atrium (LA)
P_{2f}	Left Ventricle (LV)
P_{3f}	Aorta (A)
P_{4f}	Systemic Arteries (SA)
P_{5f}	Systemic Arterioles (SAR)
P_{6f}	Systemic Capillaries (SC)
P_{7f}	Systemic Veins (SV)
P_{8f}	Vena Cava (VC)
P_{9f}	Right Atrium (RA)
P_{10f}	Right Ventricle (RV)
P_{11f}	Pulmonary Artery (PA)
P_{12f}	Pulmonary Arteries (PAS)
P_{13f}	Pulmonary Arterioles (PAR)
P_{14f}	Pulmonary Capillaries (PC)
P_{15f}	Pulmonary Veins (PVS)
P_{16f}	Pulmonary Vein (PAV)

T_{DF}	*Continuous Dynamics*
T_{1f}	Calculation of Q_{AV}, P_{LV}
T_{2f}	Calculation of Q_A, P_A
T_{3f}	Calculation of Q_{SA}, P_{SA}
T_{4f}	Calculation of Q_{SAR}, P_{SAR}
T_{5f}	Calculation of Q_{SC}, P_{SC}
T_{6f}	Calculation of Q_{SV}, P_{SV}
T_{7f}	Calculation of Q_{VC}, P_{VC}
T_{8f}	Calculation of Q_{TV}, P_{RA}
T_{9f}	Calculation of Q_{PV}, P_{RV}
T_{10f}	Calculation of Q_{PA}, P_{PA}
T_{11f}	Calculation of Q_{PAS}, P_{PAS}
T_{12f}	Calculation of Q_{PAR}, P_{PAR}
T_{13f}	Calculation of Q_{PC}, P_{PC}
T_{14f}	Calculation of Q_{PVS}, P_{PVS}
T_{15f}	Calculation of Q_{PAV}, P_{PAV}
T_{16f}	Calculation of Q_{MV}, P_{LA}

P_D	*Discrete Events*
P_1	Mitral Valve (Closed)
P_2	Mitral Valve (Open)
P_3	Aortic Valve (Closed)
P_4	Aortic Valve (Open)
P_5	Tricuspid Valve (Closed)
P_6	Tricuspid Valve (Open)
P_7	Pulmonary Valve (Closed)
P_8	Pulmonary Valve (Open)
P_9	Synchronization between T_1 and T_5
P_{10}	Synchronization between T_3 and T_7

T_D	*Discrete Events*
T_1	Open Mitral Valve (MV)
T_2	Close Mitral Valve
T_3	Open Aortic Valve (AV)
T_4	Close Aortic Valve
T_5	Open Tricuspid Valve (TV)
T_6	Close Tricuspid Valve
T_7	Open Pulmonary Valve (PV)
T_8	Close Pulmonary Valve

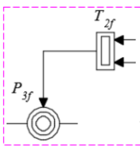

$$T_{2f} : \dot{X} = \begin{cases} \dot{x}_1 = \dfrac{dP_A}{dt} = \dfrac{Q_{AV} - Q_A}{C_A} \\ \dot{x}_2 = \dfrac{dQ_A}{dt} = \dfrac{P_A - P_{SA} - R_A Q_A}{L_A} \end{cases}$$

$$P_{3f} : X = \begin{cases} x_1 = P_A \\ x_2 = Q_A \end{cases}$$

Fig. 4. Modelling of the human cardiovascular system by Differential Hybrid Petri Net.

3. RESULTS AND DISCUSSION

In order to evaluate the capability of the proposed model to emulate the HCS hemodynamics, tests are performed by simulation using Matlab®/Simulink. These numerical simulations ignore the effects of gravity; one may hence assume that blood flows solely in response to pressure gradients. In addition, the four heart valves were simulated with the traditional on–off valve model. Thus, the normal reverse flow in the heart valves, following valve closure, is not presented in the results. In addition, normal functioning and abnormal situations, such as the aortic blockage generated by atherosclerosis or thrombosis, were simulated with the proposed model. However, due to lack of space, only the results of the normal functioning of the HCS are presented here.

Figure 5 shows the left cardiac cycle from clinical data (Guyton and Hall, 2011).

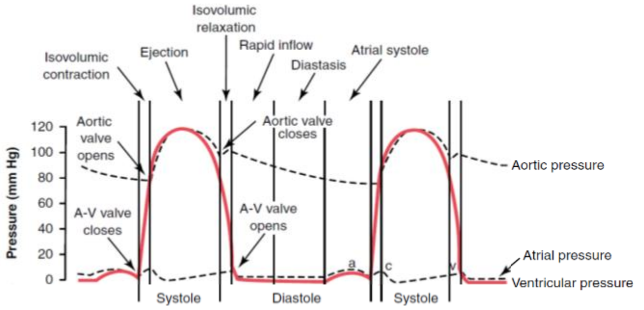

Fig. 5. Left cardiac cycle from clinical data.

Figure 6 shows simulated hemodynamic waveforms throughout the HCS model. The comparison of the numerical simulation for the left cardiac cycle (Fig. 6(a)) with clinical data (Fig. 5) shows good agreement. Moreover, the results for the right cardiac cycle and flow rate into the heart and the systemic and pulmonary circulation are in agreement with corresponding human data found in the literature (Noordergraaf, 1978; Korakianitis and Shi, 2006a, 2006b; Ferreira et al., 2005; Blanco and Feijóo, 2010; Nichols, O'Rourke and Vlachopoulos, 2011; Guyton and Hall, 2011; Frisiello et al., 2015; Mynard and Smolich, 2015; Bakir et al., 2018).

Therefore, the results are consistent with clinical data and related papers, and indicate the validity of the proposed model for the HCS by using the hybrid system approach and DHPN as a modelling technique.

4. CONCLUSIONS

This work proposed a model for the human cardiovascular system (HCS), by applying the formalism of the Differential Hybrid Petri Net (DHPN), since this formalism takes into account the concept of hybrid systems for a more detailed characterization of the cardiovascular system functioning. This model was implemented in Matlab®/Simulink.

The numerical simulations show simulated hemodynamic waveforms throughout the cardiovascular system model. The results are consistent with clinical data and related papers, indicating the validity of the proposed model for the human cardiovascular system. Thus, the application of the formalism DHPN to model the HCS allows a better analysis of the behaviour of this system, when taking into account the combination between continuous and discrete parts.

Future works will consider replacing the traditional on–off valve model by dynamic valves and including events, such as variations in the body positions and the cardiovascular diseases, to analyse the simulated hemodynamic throughout in the HCS model compared with clinical data and related papers.

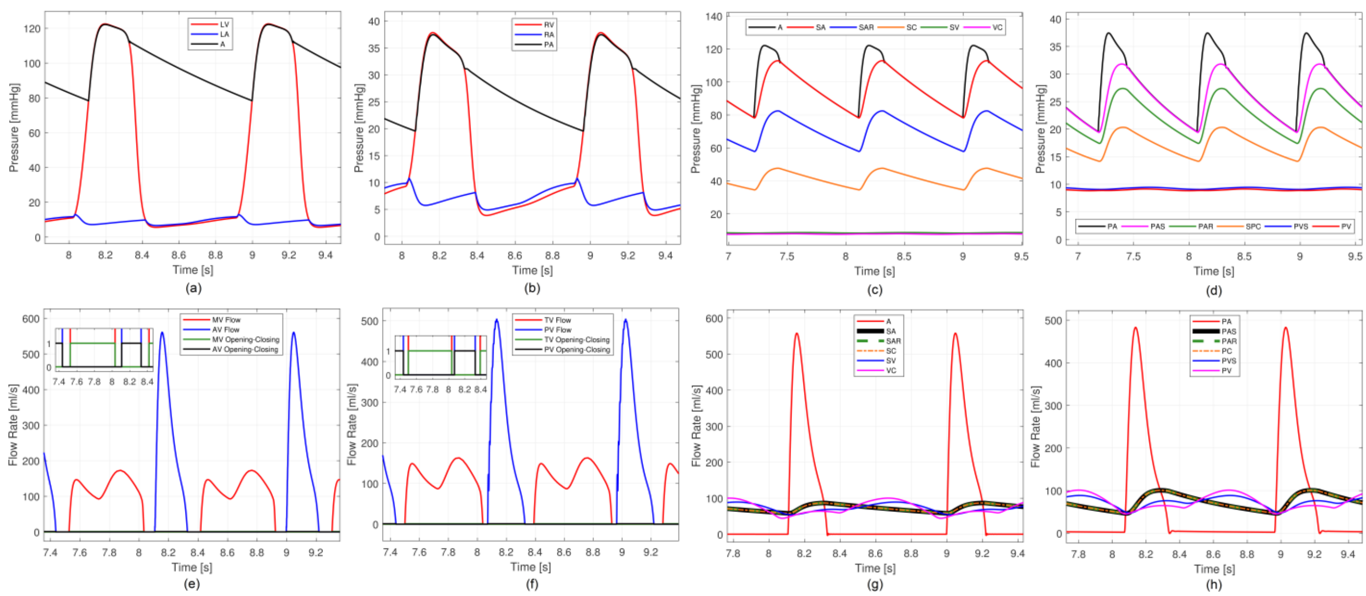

Fig. 6. Numerical simulations of the cardiovascular system model. (a) Left cardiac cycle. (b) Right cardiac cycle. (c) Pressures systemic circulation. (d) Pressures pulmonary circulation. (e) Flow rate and opening/closing of the mitral and aortic valves (left heart). (f) Flow rate and opening/closing of the tricuspid and pulmonary valves (right heart). (e) Flow rates in the systemic circulation. (f) Flow rates in the pulmonary circulation.

ACKNOWLEDGEMENT

The authors gratefully acknowledge the financial support provided by the Coordenação de Aperfeiçoamento de Pessoal de Nível Superior - Brasil (CAPES) - finance code 001, grant#2013/24434-0, Sao Paulo Research Foundation (FAPESP) and Brazilian National Council of Scientific and Technological Development (CNPq).

REFERENCES

Bakir, A. A., Abed, A. A., Stevens, M. C., Lovell, N. H. and Dokos, S. (2018). A Multiphysics Biventricular Cardiac Model: Simulations with a Left-Ventricular Assist Device. *Frontiers in Physiology*, vol. 9, n° 1259.

Blanco, P. J. and Feijóo, R. A. (2010). A 3D-1D-0D Computational Model for the Entire Cardiovascular System. *Asociación Argentina de Mecánica Computacional*, vol. 29, pp. 5887-5911.

Boussif, A. and Ghazel, M. (2018). A Diagnosis Study on a Train Passenger Access System using Petri Net Models. *International Federation of Automatic Control (IFAC)*, vol. 51, pp. 150-155.

David, R. and Alla, H. (2010). *Discrete, Continuous, and Hybrid Petri Nets*. Second edition, Springer-Verlag, Berlin.

Ferreira, A., Chen, S., Simaan, M. A., Boston, F. J. and Antali, J. F. (2005). A Nonlinear State-Space Model a Combined Cardiovascular System and a Rotary Pump. *44th IEEE Conference on Decision and Control*, pp. 897-902.

Fresiello, L., Ferrari, G., Di Molfetta, A., Zielinski, K., Tzallas, A., Jacobs, S., Darowski, M., Kozarski, M., Meyns, B., Katertsidis, N. S., Karvounis, E. C., Tsipouras, M. G. and Trivella, M. G. (2015). A cardiovascular simulator tailored for training and clinical uses. *Journal of Biomedical Informatics*, vol. 57, pp. 100-112.

Formaggia, L., Quarteroni, A. and Veneziani, A. (2009). *Cardiovascular mathematics - modeling and simulation of the circulatory system*. Springer, Milan.

Giua, A. and Silva, M. (2017). Modeling, analysis and control of Discrete Event Systems: Petri net perspective. *International Federation of Automatic Control (IFAC)*, vol. 50, pp. 1772-1783.

Gul, R. (2016). Mathematical modeling and sensitivity analysis of lumped-parameter model of the human cardiovascular system. Ph.D. thesis, University of Berlin, Berlin.

Guyton, A. C. and Hall, J. E., 2011. *Textbook of Medical Physiology*. 12th ed., Elsevier Health Sciences.

Jorge, A. A., Junqueira, F., Santos Filho, D. J. and Miyagi, P. E. (2019a). Modeling of the Human Cardiovascular System: Analysis of the Blood Flow Rate. *25th ABCM International Congress of Mechanical Engineering (COBEM)*, Uberlandia - MG.

Jorge, A. A., Riascos, L. A. M., Junqueira, F., Santos Filho, D. J. and Miyagi, P. E. (2019b). "Model of the Human Cardiovascular System based on Hybrid Systems*". 6th IEEE/SMC International Conference on Control, Decision and Information Technologies (CODIT)*, Paris.

Jorge, A. A., Ribeiro, S. A., Junqueira, F., Santos Filho, D. J. and Miyagi, P. E. (2018). Human blood circulatory system modeling based on hybrid systems. *13th IEEE/IAS International Conference on Industry Applications (INDUSCON)*, Sao Paulo - SP.

Korakianitis, T. and Shi, Y. (2006a). Numerical simulation of cardiovascular dynamics with healthy and diseased heart valves. *Journal of Biomechanics*, vol. 39, pp. 1964-1982.

Korakianitis, T. and Shi, Y. (2006b). A concentrated parameter model for the human cardiovascular system including heart valve dynamics and atrioventricular interaction. Medical Engineering & Physics, vol. 28, pp. 613-628.

Malatos, S., Raptis, A. and Xenos, M. (2016). Advances in Low-Dimensional Mathematical Modeling of rhe Human Cardiovascular System. *Journal of Hypertension and Management*, vol. 2, pp. 1-10.

Mynard, J. P. and Smolich, J. J. (2015). One-Dimensional Haemodynamic Modeling and Wave Dynamics in the Entire Adult Circulation. *Biomedical Engineering Society*, vol. 43, pp. 1443-1460.

Nichols, W., O'Rourke, M. F. and Vlachopoulos, C. (2011). *McDonals's Blood Flow in Arteries: Theoretical, Experimental and Clinical Principles*. 6th ed., CRC Press.

Noordergraaf, A. (1978). *Circulatory System Dynamics*. Academic Press, San Diego, CA.

Rahman, S. and Haque, A. (2012). Mathematical modeling of blood flow. *International Conference on Informatics, Electronics & Vision (ICIEV)*, pp. 672-676.

Shi, Y., Lawford, P. and Hose, R. (2011). Review of zero-D and 1-D models of blood flow in the cardiovascular system. *Biomedical Engineering*, vol. 10, n° 33.

Sousa, J. R. B. and Lima, A. M. N. (2008). Modeling and Simulation of Systems of Multiple Sources of Energy by Differential Hybrid Petri Nets. *International Symposium on Industrial Electronics*, pp. 1861-1866.

Tortora, G. J. and Derrickson, B. (2014). *Principles of Anatomy and Physiology*. 14th ed., Wiley.

Villani, E., Miyagi, P. E. and Valette, R. (2007). *Modelling and analysis of hybrid supervisory systems: a Petri net approach*. Springer Science & Business Media, London, England.

Watanabe, M., Fonseca, C. D. and Vattimo, M. F. F. (2014). Instrumental and Ethical aspects of experimental research with animal models. *Journal of School of Nursing - University of Sao Paulo*, vol. 48, pp. 173-183.

Westerhof, N., Stergiopulos, N. and Noble, M. I. M. (2005). *Snapshots of Hemodynamics*. Springer, US.

World Health Organization (WHO) (2017). Cardiovascular diseases. 05 Nov. 2019 <https://www.who.int/news-room/fact-sheets/detail/cardiovascular-diseases-(cvds)>.

Yobing, S. (2013). Lumped parameter modeling of cardiovascular system dynamics under different healthy and diseased conditions. Ph.D. thesis, University of Sheffield, South Yorkshire.

Yu, J., Dou, C. and Li, X. (2016). MAS-Based Energy Management Strategies for a Hybrid Energy Generation System. *International Symposium on Industrial Electronics*, vol. 63, pp. 3756-3764.